Master in Bioengineering
Specialization in Biological Engineering

NAMs' Membrane Permeabilization and Partition into Membrane Models

Master's Dissertation

Raquel Moreira da Silva

Developed within the scope of the Dissertation's curricular unit

Supervisor: Rita S. Santos, PhD
Co-supervisor: Beatriz T. Magalhães, MsC

Department of Chemical Engineering
June 2023

“The results suggest a helical structure which must be very closely packed containing probably 2,3 or 4 coaxial nucleic acid chains per helical unit and having the phosphate groups near the outside.”

Rosalind Franklin, 1952

Acknowledgements

This work was financially supported by LA/P/0045/2020 (ALiCE), UIDB/00511/2020 and UIDP/00511/2020 (LEPABE), funded by national funds through FCT/MCTES (PIDDAC).

Foremost, I would like to express my gratitude to my Supervisors Doctor Rita Sobral Santos and Beatriz Magalhães, for their invaluable advice and guidance provided throughout the project.

Additionally, I thankfully acknowledge the support of the Department of Chemistry of the Faculty of Sciences of the University of Porto, especially Professor Paula Gameiro and Doctor Mariana Ferreira for their contribution. I extend my thanks to Diogo Pereira, and Professor Luís Arnaut of the Department of Chemistry of the Faculty of Sciences of University of Coimbra for their collaboration as well as the Faculty of Pharmacy of University of Porto. I also thank to CEFT- FEUP for the use of the spin-coater.

Personally, I would like to thank my family for all the support and encouragement throughout this research work.

Abstract

In response to the antimicrobial resistance crisis, Nucleic Acid Mimics (NAMs) are potential substitutes for the traditional antibiotics, as long as they are able to efficiently cross the bacterial envelope. Therefore, studying their internalization into bacteria becomes an important milestone in the path towards the future use of NAMs as effective antimicrobials. However, internalization occurs at the nanometer scale, which makes the visual inspection of the diffusion of NAMs across the bacterial membranes a challenging task. Model membranes, such as liposomes, can be used to mimic lipidic membranes and thus enable the characterization of permeation in bacteria.

In the present work, NAMs' permeabilization and partition towards lipidic membranes was assessed through a variety of methods, including biochemical, microscopic, and spectroscopic methods. Firstly, the composition of liposomes to mimic the bacterial inner membrane was studied, using brightfield microscopy. After this, epifluorescence microscopy assays were performed to assess if fluorescently labelled NAMs could internalize the liposomal vesicles. It was observed that when using higher concentrations (15, 30 and 60 μM), NAMs were able to diffuse into the vesicles. Spectroscopic assays were also conducted to further investigate NAMs interaction with the membrane, and its lipid composition. For the Partition assay, there seemed to be a slightly higher interaction with PG vesicles than PC vesicles, due to its anionic charge. Permeabilization assays results for NAMs showed high variation intraassay.

Conclusions show that NAMs internalization in liposomes could be visualized (with the higher concentrations used) to some extent but its interaction, partition and permeabilization, with anionic and zwitterionic vesicles point to little to none interaction with the membrane. Future work includes the study of carriers for increased internalization.

Key Words Nucleic Acid Mimics, Liposomes, Bacterial membrane, Membrane Permeabilization and Partition

Resumo

Em resposta à crise de resistência antimicrobiana, os Mímicos de Ácidos Nucleicos (NAMs) são potenciais substitutos dos antibióticos tradicionais, desde que possuam a capacidade de atravessar eficientemente o envelope bacteriano. Portanto, estudar a sua internalização em bactérias torna-se importante no caminho para o uso futuro de NAMs como antimicrobianos eficazes. No entanto, a internalização ocorre na escala nanométrica, o que torna a inspeção visual da difusão de NAMs através das membranas bacterianas uma tarefa desafiante. Membranas modelo, como lipossomas, podem ser usadas para imitar membranas lipídicas e, assim, permitir a caracterização da permeabilização em bactérias.

No presente trabalho, a permeabilização e partição de NAMs de membranas lipídicas foi avaliada através de vários métodos, incluindo métodos bioquímicos, microscópicos e espectroscópicos. Em primeiro lugar, a composição dos lipossomas, para se assemelharem à membrana interna bacteriana, foi estudada, usando microscopia. Depois disso, ensaios de microscopia de epifluorescência foram realizados para avaliar se NAMs marcados com fluorescência poderiam internalizar as vesículas. Observou-se que, ao utilizar concentrações mais elevadas (15, 30 e 60 μM), os NAMs foram capazes de se difundir para as vesículas. Ensaios espectroscópicos também foram conduzidos para investigar a interação dos NAMs com a membrana e sua composição lipídica. Para o ensaio de partição, pareceu haver uma interação ligeiramente maior com as vesículas PG do que com as vesículas PC, devido à sua carga aniónica. Os ensaios de permeabilização para NAMs mostraram alta variação intra ensaio.

Mostrou-se que a internalização de NAMs em lipossomas pode ser visualizada (com as maiores concentrações utilizadas) até certo ponto, mas a sua interação, partição e permeabilização, com vesículas aniónicas e zwitteriónicas, aponta para pouca ou nenhuma interação com a membrana. O trabalho futuro inclui o estudo de transportadores para uma maior internalização.

Palavras-Chave Mímicos de Ácidos Nucleicos, Lipossomas, Membrana Bacteriana Interna, Permeabilização e Partição de Membranas

Declaration

Declares, under oath, that this work is original and that all non-original contributions have been duly referenced with identification of the source.

Porto, 16 of June 2023

Index

I. Notation

ANTS/DPX	Aminonaphthalene trisulfonic acid/ p-xylene-bis-pyridinium bromide
CPX	Ciprofloxacin
DLS	Dynamic light scattering
EDTA	Ethylenediaminetetraacetic acid
FQ	Fluoroquinolone
GUV	Giant unilamellar vesicle
I_0	Fluorescence intensity without addition of drug
I_M	Inner Membrane
I_t	Fluorescence intensity after addition of drug
I_{tot}	Fluorescence intensity after complete vesicle permeabilization
K_p	Partition Coefficient
LNA	Locked Nucleic Acid
LPS	Lipopolysaccharide
LUVs	Large unilamellar vesicles
MLVs	Multilamellar vesicle
MV	Methyl Viologen
NAMs	Nucleic Acid Mimics
OLVs	Oligolamellar vesicle
OM	Outer Membrane
OS	Phosphatidylserine
PC	Phosphatidylcholine
PE	Phosphatidylethanolamine
PG	Phosphatidylglycerol
PI	Phosphatidylinositol
PMB	Polymyxin-B-Rhodamine B
PNA	Peptide Nucleic Acid
PTS	1,3,6,8-pyrenetetrasulfonic acid tetrasodium salt
PVA	Polyvinyl alcohol
SD	Standard Deviation
SMs	Sphingomyelins

SUV	Small unilamellar vesicle
γ_L	Molar volume of the lipid
Δp	Variation of the spectroscopic signal measured ($\mathrm{p}_{observed} - \mathrm{p}_{water}$)
$\Delta \mathrm{p}_\infty$	Maximal variation of the signal ($p_{lipid} - p_{water}$)

II. List of Figures

III. List of Tables

1. Introduction

1.1 Antibacterial Resistance

Antibacterial Resistance was found more than 50 years ago, and is, to this day, one of the most serious causes of morbidity and mortality, threatening to rise within the next few decades [1, 2]. In fact, it is estimated that, in 2019, 1.27 million deaths were caused by antibacterial resistance directly, and it is argued that it could kill 10 million people per year by 2050 [3].

This natural phenomenon occurs when the antibiotic or antimicrobial drug is used in the presence of microorganisms and imposes a selective pressure. Under this pressure, susceptible microorganisms are eliminated and bacteria that are resistant, either by intrinsic resistance, acquired resistance, or other, are selected, being able to survive, multiply and spread [4, 5].

Intrinsic resistance is a mechanism developed by bacteria in order to survive and overcome antimicrobial compounds naturally produced by co-resident bacteria. Acquired resistance is where the resistance conundrum lies, as bacteria that was originally susceptible becomes resistant. This can be through mutation or transference of genes for resistance traits among bacteria of different taxonomic and ecological groups, with mobile genetic elements (bacteriophages, plasmids, DNA, or transposons). The resistance trait is most commonly affecting one single family of antibiotic, although different genes, each with a different resistance trait, can exist in the same organism [5, 6]. The clinical problem is enhanced by the millions of kilograms used each year in prophylaxis or treatment of people, animals and agriculture, selecting the resistant strains [5].

Antibiotics mechanisms of action are wide but can be summed up to: Inhibition of cell wall (e.g., penicillin, daptomycin), protein (e.g., tetracyclines), of DNA (e.g., fluoroquinolones, in particular, ciprofloxacin (CPX)) or RNA synthesis (e.g., Rifampin) and competitive inhibition of folic acid synthesis (e.g., sulfonamides, trimethoprim) [5]. Besides the antibiotics that

act at the bacterial envelope, the remaining ones have intracellular targets. This derives from the fact that they are small-molecules able to translocate the bacterial envelope.

1.2 Nucleic acid mimics

Fluorescent *in situ* hybridization (FISH) is a technique that allows the detection, quantification and localization of DNA and RNA sequences in cells or tissues. For this, complementary nucleotide probes labelled with a reporter molecule bind to a specific target nucleic acid sequence. Nucleic acid mimics (NAMs) were introduced in FISH given their increased stability and affinity to RNA, allowing improved hybridization efficiency with the target [7].

To elaborate, NAMs are chemically and structurally modified DNA or RNA chains, such as the peptide nucleic acid (PNA) and the locked nucleic acid (LNA), that also obey the Watson- Crick base-pairing rules [8, 9]. Some of the key features of NAMs include their increased affinity, sensitivity, and specificity towards the target, as well as nuclease resistance [7, 10]. The configuration of these sequences is identical to that of natural DNA, as the nucleobases are practically positioned within the same distance, which allows for the mentioned hybridization with complementary DNA or RNA sequences [10].

The modifications can be present in the nucleobase, the sugar ring, or the phosphodiester backbone [11]. PNA probes were first described by Nielsen et al. in 1991 [12], as a DNA mimic with a neutral polyamide backbone, instead of a negatively charged sugar-phosphate backbone, composed of repetitive unites of N-(2 aminoethyl) glycine. The nucleobases are attached via methylene carbonyl linkers, instead of negatively charged sugar phosphates. LNA was invented by Obika *et al*. and Koshkin *et al*. in 1997 and derive from synthetic RNA, containing a ribose ring locked by a 02'-C4'-methylene linkage [13]. The 2'-0-methyl modifications is a common second generation modification of RNA, which consists of a methyl group added to the 2' hydroxyl of the ribose moiety of a nucleoside [14].

Taking this into consideration, NAMs' capacity for microbial cell growth inhibition is being studied. This can be achieved by using antibacterial antisense therapy, in which NAMs are designed to be complementary to an essential gene, leading to cell death upon hybridization, or to a gene that confers resistance to antibiotics, reverting such bacterial resistance. If any microbial resistance emerges, by point mutations, the antisense technology allows to easily redesign the NAM sequence in order to provide an effective drug again, promising a theoretical endless source of active antibacterial drugs. This is one of the major advantages of using NAMs as opposed to classic antibiotics [8, 9]. However, differently from classic antibiotics, NAMs are biological drugs, and it is thus critical to understand if they are able to cross the bacterial envelope and internalize into the bacterial cytosol where they should hybridize with the target sequence. With this in mind, the diffusion of NAMs across the multi-layered envelope of bacteria is a key point to be studied, either by passive diffusion or with the development of carriers, either peptides, liposomes, or others [15, 16].

1.3 Bacterial envelope

The multi-layered envelope of bacteria is a complex structure that defines the boundaries of the bacterial cells, conferring protection from the environment and permitting selective passage of nutrients. Christian Gram, through a staining procedure, was able to classify bacteria in two categories: the ones that retain stain and become blue or purple, Gram-positive, and the ones that do not and become pink or red, Gram-negative [17]. The main differences can be seen Figure 1.

Gram-negative cell envelopes are composed of an outer membrane (OM), an aqueous compartment dubbed periplasm that contains the peptidoglycan cell wall, and the cytoplasmic or inner membrane (IM) [17].

The OM is a lipid bilayer, with the inner leaflet composed of phospholipids and the outer leaflet composed of lipopolysaccharide (LPS). The OM has proteins such as lipoproteins, porins and others for the passive diffusion

of small molecules, including mono and disaccharides, and amino acids and others [17].

The peptidoglycan cell wall is a rigid exoskeleton, composed of repeated units of disaccharide N-acetyl glucosamine-N-acetyl muramic acid, cross-linked by pentapeptide side chains [18].

The IM is a phospholipid bilayer, where many functions occur as bacteria lack intracellular organelles, such as the production of energy, synthesis of lipids, protein secretion and others. In *E.coli* the main phospholipids present are phosphatidylethanolamine (PE) and phosphatidylglycerol (PG), making up 75% and 20% of the composition of the membrane [17]. The remaining 5% consists of other lipids (e.g., cardiolipin) [17].

Gram-positive cell envelopes also have the IM, with similar properties to the Gram-negative cells' IM but lack the protection of an OM. To counteract this, the peptidoglycan mesh is many times thicker than the one found in Gram-negative cells [17]. This can be seen in Figure 1.

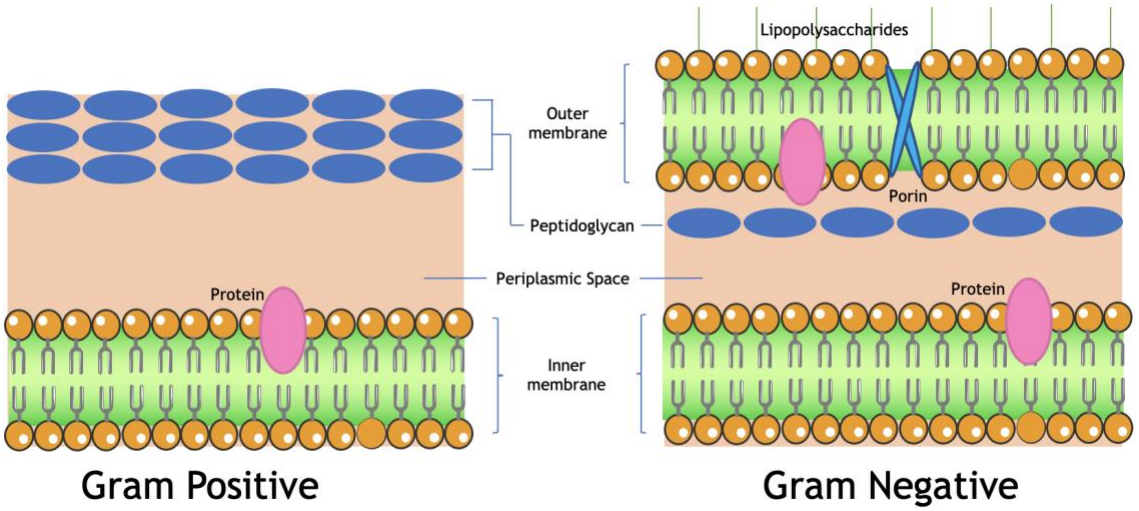

Figure 1: Schematic representation of Gram Positive and Negative envelopes, depicting the Inner membrane, Periplasmic Space, Peptidoglycan wall and Outer membrane. This image was made using pictures from Servier Medical Art.

The lipidic bilayer is composed of two adjacent layers of phospholipids, which form spontaneously in aqueous solutions, with the hydrophobic tails facing the interior and the polar head the exterior of the membrane. These membranes behave as a two-dimensional fluid, as the constituent lipids and

proteins can laterally rotate and move. Therefore, fluidity is an important property of membranes, which can be influenced by temperature and lipid composition [19].

This organization creates a semipermeable membrane, which allows the passage of uncharged small molecules, while being impermeable to larger polar molecules. For these to be able to cross the membrane, there must be a specific transmembrane protein for the process. Two classes of membrane transport proteins exist: Channel proteins and Carrier proteins [19]. While Channel proteins form aqueous pores to allow the diffusion, Carrier proteins bind to the solute so it can be transported. It is also possible that membrane traffic happens by endo and exocytosis [20, 21].

1.4 Phospholipids

Phospholipids have an amphiphilic nature, due to their structure being composed of a hydrophilic moiety and hydrophobic fatty acid chains. Phospholipids are found naturally in all living organisms and compose the majority of cell membranes [22].

This class of lipids can be subdivided into glycerophospholipids and sphingomyelins (SMs), according to the alcohol group contained. Glycerophospholipids have glycerol as the backbone and possess α-structure and L-configuration; variation in the head group creates different lipids, including phosphatidylcholine (PC), PE, phosphatidylserine (PS), PG, phosphatidylinositol (PI). Sphingomyelins differ in the backbone, as this is composed of sphingosine, opposed to glycerol [23, 24].

Phospholipids can also be divided into natural and synthetic phospholipids. Natural phospholipids can be found in vegetable oils and animal tissues, whereas synthetic phospholipids can be obtained by semi-synthesis or total synthesis [23, 25]. The semi-synthesis process involves changing the chemical structure of a natural phospholipid, for example the head, tail group, or both. The total synthesis process is more complex: starting with a glycerol

backbone, ester or ether bonds link the nonpolar moieties and polar head group [26].

As aforementioned, phospholipids are naturally present in cell membranes. However, they can organize themselves in different ways: from micelles to a liposomal bilayer. In the present work, a special focus will be given to liposomes, vesicles commonly used as mimics of cellular lipidic membranes.

1.5 Liposomes as Model Membranes

Liposomes arrange themselves in a vesicular and spherical shape. Their amphiphilic nature allows the formation of a bilayer or of multiple layers, called uni or multilamellar.

Size and number of bilayers classifies liposomes in the following way: Small unilamellar vesicles (SUVs): 20-100 nm; Large unilamellar vesicles (LUVs): >100 nm; Giant unilamellar vesicles (GUVs): >1000 nm; Oligolamellar vesicle (OLVs): 100-500 nm; Multilamellar vesicle (MLVs): >500 nm [27, 28].

Importantly, liposomes are commonly used as models for lipidic membranes, as they are easy to prepare, and their size and composition can be defined according to the protocol followed [29-31].

Liposomes can be prepared with natural and/or synthetic phospholipids (PE, PG, PC, PS, and PI). Different methods of liposome preparation have been developed, taking into consideration the size, charge, structure, and desired application. These methods can be divided based on the technique used, that is, if they use mechanical agitation, solvent evaporation, solvent injection or detergent solubilization [32].

The first preparation method described was the Bangham method or thin lipid film hydration method [32]. The formation of a film of phospholipid is created through evaporation of the organic solvent, in which they were solubilized. Freezing of the film assures the total removal of the solvent.

Rehydration with aqueous solvents sues, and liposomes form. This method creates a heterogeneous size distribution and mainly MLVs. SUVs can be achieved by sonication or extrusion of the final product [32, 33].

Another conventional method is reverse phase evaporation. Lipidic films are formed through the evaporation of the solvent, then purged with nitrogen and re-dissolved in another organic phase (usually diethyl ether or isopropyl ether). An aqueous phase is added, and the organic solvent is then removed. The result is liposomes with a high encapsulation efficiency [33, 34].

The conventional methods are easy to follow but require large amounts of organic solvent (harmful to the environment and health) and energy. With mass production in mind, other methods of industrial scale production have been developed, such as: Heating method, Spray drying, Freeze drying, and Super Critical Reverse Phase Evaporation [27, 33, 34].

In this project, liposomes (GUVs and LUVs) were prepared by the thin lipid film hydration method and used. These are simple model membrane systems, which are instrumental in the study of complex biological membranes, and offer high entrapment of hydrophilic material [35].

1.6 Methods to study permeation of liposomes as model membranes

1.6.1 Partition Coefficient (K_p)

An important parameter to predict the ability of compounds to cross biological membranes through passive diffusion is the partition coefficient (K_p) [36]. The K_p is defined as the concentration ratio of a molecule between two media at equilibrium. Different methods can be used to determine this parameter experimentally, depending on the media being used [37].

In liposomes, the determination of the K_p is typically done by employing spectrophotometric methods. Steady-state fluorescence and time-resolved spectroscopy can be used when the molecule has autofluorescence or by

tagging it to a fluorochrome. Upon addition of the molecule under study to the liposome solution, a shift occurs, resulting in signal quenching or enhancement, depending on the specific change of the dipole moment of the molecule. This signal variation can be plotted and fitted to an appropriate equation. The concavity of the curve changes according to the quenching or enhancement of the signal with increasing lipid concentrations (Figure 2). If there is no partition between the molecule and the lipid, no shift occurs, and the plot will reveal constant slope. [38]

In the UV-VIS determination method, the background signal often obstructs the direct application of the method. To solve this, derivative spectrophotometry can be used, which sharpens the signals, improving the resolution. This allows to measure a spectral change upon the molecule/lipid interaction, and consequently the determination of K_p, without taking extra steps as time-consuming separation of phases [36, 38].

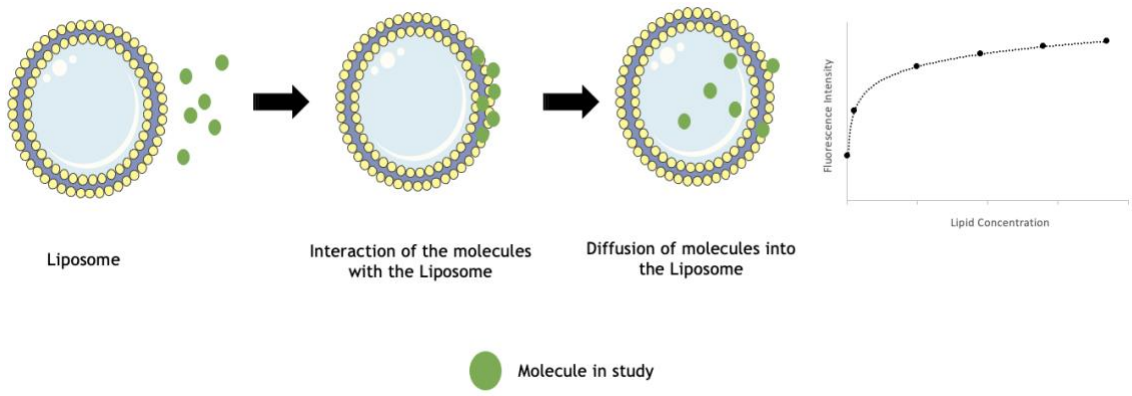

Figure 2: Schematic of partition of a Molecule in study in LUVs and example graph for a fluorescence enhancement with increasing amounts of lipid. This image was made using pictures from Servier Medical Art.

Partition assays' methodology has been employed with a large variety of drugs and using different lipids. Daunorubicin is a natural antitumoral drug, which has been studied to determine its way of action: K_p was determined using derivative spectrophotometry and zeta-potential evaluation, and the result showed an inner partition dependent of the membrane structure and lipid composition [39]. Several classes of antibiotics have also been studied using

Langmuir monolayers, revealing different behaviours for each antibiotic, with hydrophobicity being a desirable feature for insertion in LPS [40]. Grepafloxacin is second-generation fluoroquinolone, with enhanced efficiency; studies have been conducted to determine its' K_p, through quenching and Steady-State Anisotropy Experiments, to reveal the importance of charge interactions, and show that the molecule can have increased therapeutic activity due to the charge interaction between the drug and the membrane surface [41]. Partition assays have also been employed to study the difference between ionized hydrophilic and hydrophobic contributions for the formation of the drug-lipid interaction [42]. These examples can be seen in Table 1 below.

Table 1: Examples of results of Partition assays from the literature.

Lipid	Vesicule	Molecule	K_p	Reference
PC	LUVs	Daunorubicin	1.08	[39]
LPS	Langmuir monolayers	Novobiocin	5.63	[40]
		Rifampicin	6.54	
		Azithromycin	5.75	
		Telithromycin	5.83	
		Gentamicin	6.84	
		Polymyxin B	7.71	
		Colistin	7.76	

1.6.2 Membrane Permeability Assays

The permeability of membranes varies depending on their composition and the molecules in study [43].

Fluorescence techniques have been employed as efficient methods to monitor permeability of membranes. These methods could either be indirect, using self-quenching probes, dye/quencher pairs, lanthanide cation/ligand

pairs, or direct through visual inspection of fluorescence through fluorescence microscopy. Other methods can also be used, such as Dynamic dialysis, Dispersion method, etc.

The self-quenching method is characterized by having the fluorescent agent in the liposomal aqueous compartment at a concentration in which it is self-quenching. The membrane permeability is assessed by tracking the release of the dye and associating its' with the kinetic.

Time-lapse confocal fluorescence microscopy relies on the entry of the fluorescent dye into empty GUVs. The molecule in study must be fluorescent or tagged for the use of the microscope, which allows for the visualization of the vesicles (which must be also tagged) and the presence/lack of the molecule in study inside the vesicles through different filters, corresponding to the emission of each fluorochrome. Permeability and release kinetics can be studied through monitoring of the influx of the fluorescent dye inside the vesicle [44].

The lanthanide cation/ligand pair method is less frequently used. In this method, a weak fluorescent lanthanide cation and fluorescence enhancer ligand are co-encapsulated. High fluorescence will be detected (due to the chelation of the cation by the ligand), and, as the pair is released to the exterior, a chelator (e.g.: ethylenediaminetetraacetic acid (EDTA)) will cause fluorescence decrease by dissociating the complex. The membrane permeabilization will be assessed by measuring the fluorescence intensity, which should decrease with time due to the leakage of the probes and subsequent chelation [44].

In the dye/quencher pair method, both molecules are encapsulated within the liposome and the fluorophore's release is tracked by the increase of fluorescence, as it moves away from the quencher. A common pair used in this method is the aminonaphthalene trisulfonic acid/ p-xylene-bis-pyridinium bromide (ANTS/DPX) [44]. Another way of using the dye/quencher pair method for measuring liposomes' permeability to certain molecules is by only encapsulating the dye (e.g., 1,3,6,8-pyrenetetrasulfonic acid tetrasodium salt (PTS)), while the quencher is in the medium. Both the dye and quencher are

incapable of crossing lipidic bilayers. If the molecule in study is capable of permeabilizing the liposomes, the dye leaks out of the vesicles and comes into contact with the quencher in the medium. This allows the evaluation of the permeabilization of the membrane by relevant molecules, such as NAMs, as the leakage translates into decrease of the dye's fluorescence (Figure 3) [38, 45].

The dye/quencher pair method has been highly relied on for several permeabilization studies. To study the intrinsic apoptosis pathway, the BCL-2 family of proteins have been studied in matters of permeabilization of the

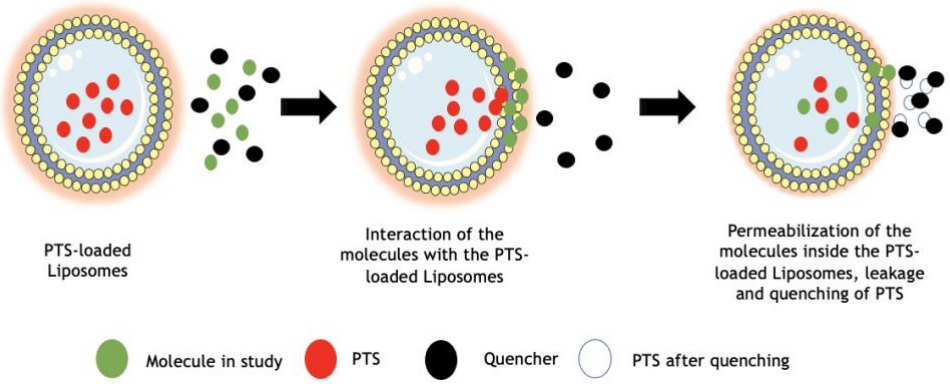

Figure 3: Schematic of dye/quencher pair method using PTS-loaded LUVs. This image was made using pictures from Servier Medical Art.

mitochondrial membrane through the dye/quencher pair method, allowing for the description in detail, in liposomes, of the interaction between the proteins and the membrane [46]. In another study, this method was employed to study the permeabilization of the antimicrobial peptide melittin, which uncovered that the leakage could occur in separated, but successive, events, through permeabilization followed by resealing of the membrane [47]. Additionally, membrane leakage studies have also been used to test the activity of molecules such as pore-forming toxins, understanding their virulence and interaction with lipids [48]. In another field of study, this technique was employed with light-controlled release, to study enhanced drug biodistribution and bioavailability at target sites, through membrane destabilization and permeabilization [49].

The internalization, partition and permeabilization capacity of NAMs in liposomes as never been studied to the best of the author's knowledge. In this work, GUVs and LUVs were chosen as models for bacterial phospholipidic membranes to gain insights into chances and challenges for NAMs diffusion

across lipidic bilayers. Different liposome compositions were studied to evaluate the influence of phospholipidic charge and structure.

2. Materials and Methods

2.1 Lipids

Lipids used in this project were obtained from AVANTI Polar Lipids: 1-palmitoyl-2-oleoyl-sn-glycero-3-phospacholine (PC), phosphatidylglycerol (PG) and of rhodamine (rh)-phosphatidylethanolamine (PE).

2.2 Preparation of GUVs

GUVs were prepared as described by D. A. Pereira *et al.*, using the gel-assisted swelling method. Different types and concentrations of lipids were tested to optimize the formation of GUVs: 100% of PC, 100% of rh-PE, 100% of PG, 80% of rh-PE and 20% of PG, 50% of rh-PE and 50% of PG, 20% of rh-PE and 80% of PG [15].

The protocol of formation of GUVs is as follows: 200 μL of 5% (w/w) polyvinyl alcohol (PVA) in 280 mM sucrose were spin-coated (1200rpm, 120s) on the wells of an uncoated 8-well μ-slide (Falcon) and allowed to dry for 15 min at 60ºC [15].

Afterwards, with the μ-slide placed on top of a heating plate (~40ºC), 10 μL of the lipid solution in chloroform was added on the center of each well with the help of a glass syringe. The μ-slide was then placed under vacuum for 15 min in a desiccator to remove traces of solvent. The resulting lipid films were hydrated with 300 μL of 280 mM sucrose per well and protected from light for 2h.

The swelling of the lipid film leads to the formation of GUVs. By gentle agitation, they detach from the film and can be transferred to microtubes and allowed to rest for 30 min. One mL of 280mM glucose was then added to each microtube, which caused the GUVs containing sucrose, which has a higher density than glucose, to slowly deposit to the bottom of the solution. The solution was transferred to a clear polystyrene 96-well plate, and left for 30 minutes of rest [15]. Thereafter, to verify if GUVs were formed, a 10x magnitude objective on an Olympus CKX41 SF-5 microscope was used and

brightfield images were obtained. Additionally, GUVs containing PE were inspected through fluorescence using the URF LT50 filter, since PE is marked with lissamine-rhodamine, a fluorescent dye that emits fluorescence in the red spectra (with excitation/emission maxima ~560/580 nm). An analysis of the vesicle's size was made with the Fiji program, measuring the diameter, using the scale in the microscope images, for the successful formation compositions.

2.3 Preparation of NAMs solutions

NAMs were purchased from Eurogentec. Two NAM sequences were used in this study, a 14-mer oligonucleotide probe (/5'6FAM/lT*mG*mC*lC*mU*mC*lC*mC*mG*lT*mA*mG*lG*mA) and a 7-mer probe ((/5'6FAM/lTmGmClCmUmClC). Both probes were tagged with fluorescein (FAM – green fluorescence) and composed of a mixture of LNA (l) and 2'OMe nucleotides (m). Additionally, the 14-mer sequence had a PS (*) backbone modification. The target of both sequences is a complementary ribosomal RNA sequence that is universal among bacteria (i.e., binds to any eubacteria). Stock solutions at a concentration of 500 μM were prepared in sterile ultrapure water and diluted to the desired concentrations (2 μM, 10μM, 15 μM, 30 μM, and 60 μM).

2.4 Visualization of NAMs internalization in GUVs

One hundred and fifty μL of the NAMs solutions were pipetted directly into the 96-well plate with the GUVs, at room temperature. After 10 minutes of incubation, GUVs were observed using inverted Nikon epifluorescence microscope equipped with the FITC filter.

2.5 Preparation of LUVs

LUVs were prepared as described by C. F. Sousa et al., using either PC or PG. Lipid solutions were prepared in chloroform, with a concentration of 2000 μM or 25000 μM. Lipidic films were formed by drying of the chloroform, under a stream of nitrogen. To eliminate any trace of the solvent, the films were submitted to vacuum for three hours in a desiccator connected to a pump. Thereafter, MLVs were formed by redispersion of the lipidic film with HEPES buffer (10 mmol.dm3 HEPES hemisodium salt (purity 99.0 %), 0.1 mol.dm3 NaCl), provided by SIGMA- ALDRICH (pH = 7.4).

Five freeze and thaw cycles were performed, using liquid nitrogen and a water bath; these cycles increase the volume of the vesicles and decrease the number of layers. The MLVs were then extruded ten times through 100 nm WHATMAN polycarbonate filters, using an Avanti Polar Lipids extruder connected to a thermostatic water bath at 37 ºC (Figure 4). This allowed the uniformization of the vesicles' size [50], as confirmed by Dynamic light scattering (DLS), using a Zeta Sizer Nano ZS from MALVERN Instruments. Empty LUVs were used in the Partition Assays of this project. PTS-loaded LUVs were prepared following the same protocol, with the exception that the lipid films were rehydrated with 0.5 mL of PTS at a concentration of 1 mmol.dm^{-3}. Encapsulated LUVs were separated from PTS free in the solution using a Sephadex-G25 column, using HEPES as eluent. Two mL fractions were collected, and their fluorescence signal measured using a FlexStation 3 Multi-Mode Microplate Reader by setting the excitation and emission wavelengths (WLs) to 355 nm and 385 nm, respectively, to determine in which fraction the LUVs are present. It is expected that the LUVs are eluted first, resulting in a first intensity peak (~5000), and the free PTS after, resulting in a second peak of higher intensity. The fractions with maximal concentration of PTS-loaded LUVs (10 and 12) were used in Permeabilization Assays. The chromatograms are in Annex 1.

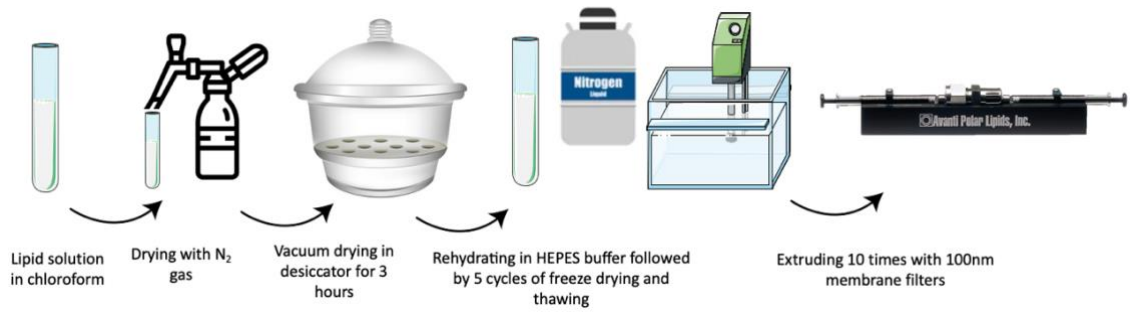

Figure 4: Schematic of LUVs' Preparation Protocol. This image was made using pictures from Servier Medical Art.

2.6 Column Preparation

The Sephadex-G25 column was prepared by adding approximately 10 mL of water to 6.5 g of Sephadex-G25 (Medium) and heating the solution in a 30 ºC water bath for 30 minutes. Afterwards, the air was removed by vacuum in a desiccator. This process was finished when the air bubbles stopped appearing. The solution was then added to an empty column (Kimble, Flex-Column), letting the water drip to a beaker. Thereafter, the column was equilibrated with 500 mL of buffer.

2.7 Partition Assays

To determine the K_p of a molecule into lipidic bilayers, spectroscopic methods can be used, if the molecule's penetration causes a change to a spectroscopic parameter in the system. For this, six samples with constant a concentration of analytes (NAMs, ciprofloxacin (CPX), and Rhodamine-B-Polymyxin-B (Rh-PMB)) of 5 µM, and increasing lipid amounts (0, 100, 200, 350, 500 and 700 µM) were prepared. The samples were incubated at 37 ºC for 30 minutes. Steady-state fluorescence was recorded for each sample in a 96-well opaque (black) plate, using a FlexStation 3 Multi-Mode Microplate Reader. This is depicted in Figure 5. For CPX, the excitation and emission WLs were set to 430 nm and 420 nm, respectively. For Rh-PMB, an excitation WL of 546 nm and an emission WL of 595 nm were used. For NAMs, the excitation WL was set to 490 nm and the emission WL to 520 nm. References with liposomes but not the analyte, and at the same concentration as in the sampled, were also prepared. Three independent assays were conducted. The fluorescence intensity of the

references was subtracted from that of the sample, to normalize the data by removing possible background noise. After this, the data was used to calculate the K_p using Equation 1.

Following C.F. Sousa *et al.*, the steady-state fluorescence was the method used in this project, with the measured parameter being the combination of signals from the molecule's population in the aqueous and lipid phases. The expression to determine the K_p is:

$$\Delta p = \Delta p_{\infty} \cdot \frac{K_p \cdot [Lipid]}{\frac{1}{\gamma_L} + K_p \cdot [Lipid]} \quad \text{(Equation 1)}$$

Where γ_L is the molar volume of the lipid and [Lipid] is its molar concentration. Δp is the variation of the spectroscopic signal measured ($p_{observed} - p_{water}$) and Δp_{∞} is the maximal variation of the signal ($p_{lipid} - p_{water}$). [51]

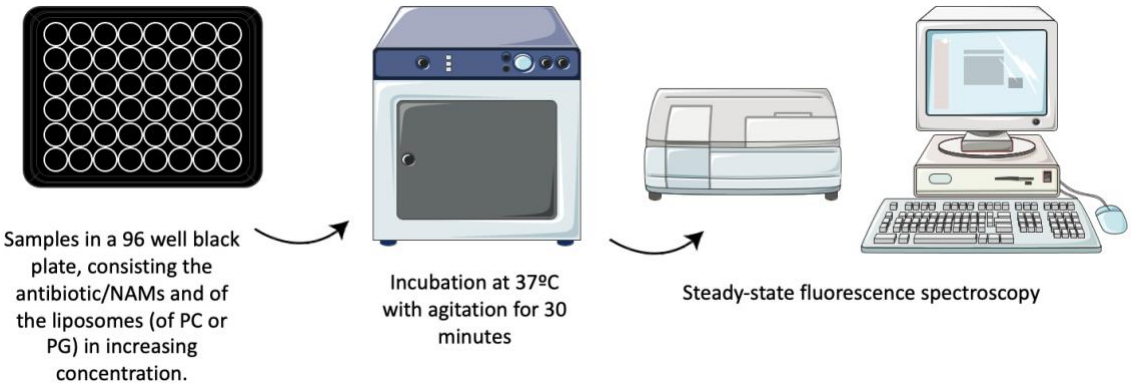

Figure 5: Schematic of the protocol for the Partition Assays. This image was made using pictures from Servier Medical Art.

2.8 Bartlett Assay

The bartlett assay is a frequently used method for the quantification of phospholipids. It is based on the acid mineralization of the phosphorus atoms in the phospholipids to inorganic phosphate. After this, it is transformed to phosphomolybdic acid by the ammonium molybdate solution, and then reduced to blue of molybdenum by addition of Fiske & Subbarow's reagent. The intensity

of the color blue is measured spectrophotometrically. This correlates to the phosphor and phospholipid concentration, as most phospholipids contain one mole of phosphor per mole of phospholipid.

Half a mL of each sample at different estimated concentrations, standard solution, or deionized water (blank) were added to glass microtubes, followed by 0.4 mL of 70% perchloric acid. The tubes were immediately incubated in a sand bath at 180 - 200ºC for 1 hour, with rigorous temperature control. The tubes were then allowed to cool down, and 4.6 mL of ammonium molybdate solution and 0.2 mL of Fiske & Subbarow's reagent were added. After being vortexed, the tubes were boiled for 7 minutes. After cooling down, 200 ml of each sample, standard solution or blank were added to a clear polystyrene 96-well plate and the absorbance was measured at 830 nm (Figure 6)[52].

Nonetheless, it was not possible to go through with such calculations, as the assay did not seem to give accurate results. The reason behind it is not clear. Hence, a direct estimate of the concentration was used, taking into account the initial concentration and volume eluted and the final volume in the aliquot (4 mL).

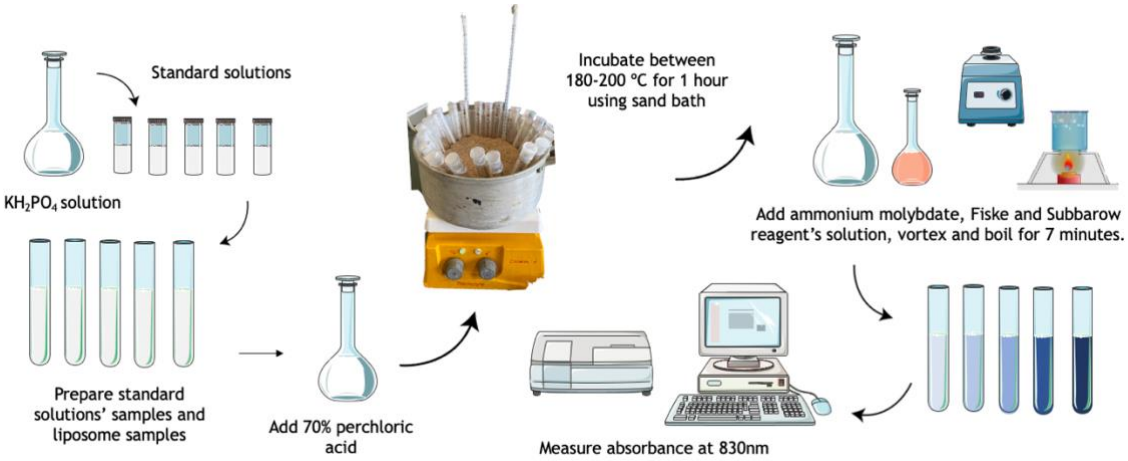

Figure 6: Schematic of Bartlett Assay. This image was made using pictures from Servier Medical Art.

2.9 Membrane Permeabilization Assays

Membrane permeabilization was evaluated through the fluorophore/quencher pair method. PTS was used as the fluorophore molecule and Methyl viologen dichloride hydrate (MV) were chosen as the fluorophore/quencher pair. Neither molecule is able to cross intact lipidic membranes. Previously produced and quantified PTS-loaded LUVs were used.

Each aliquot of the PC or PG PTS-loaded LUVs to achieve a final concentration of 200 μM were incubated with increasing concentrations of the analyte (0, 5, 10, 15, 20 μM for CPX; 0, 5, 30, 90, 200 μM for PMB, and 0, 5, 10, 15, 20 μM for NAMs) and MV at a final concentration of 1 mM, for 30 minutes at 37 ºC. References were also prepared with polidocanol, a detergent, for complete vesicle permeabilization. Three independent assays were conducted. PTS fluorescence emission was measured in a FlexStation 3 Multi-Mode Microplate Reader by setting the excitation WL to 355 nm and the emission WL to 385 nm. This is depicted in Figure 7.

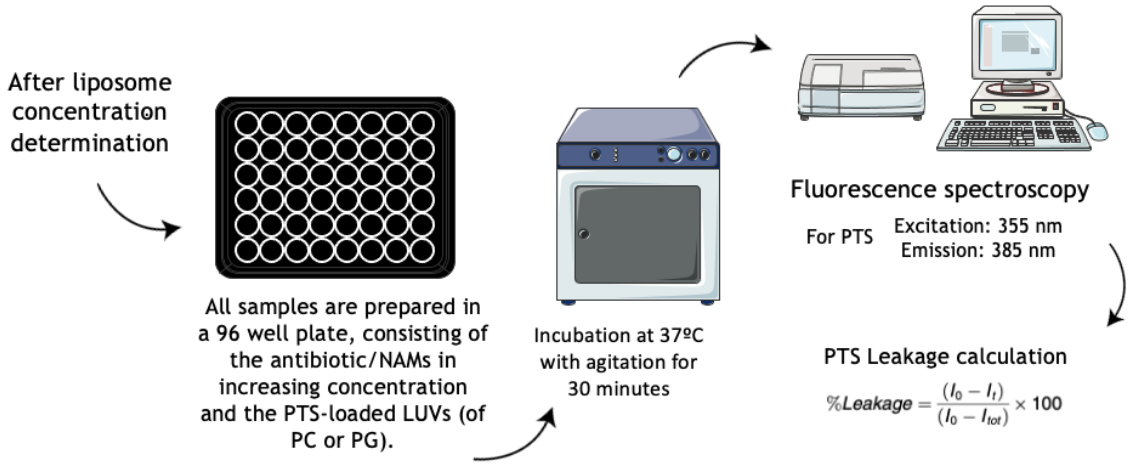

Figure 7: Schematic of the protocol for the Permeabilization Assays. This image was made using pictures from Servier Medical Art.

This allows for the calculation of the percentage of leakage, using Equation 2:

$$\%Leakage = \frac{(I_0 - I_t)}{(I_0 - I_{tot})} \times 100 \text{ (Equation 2)}$$

where I_0 is the fluorescence intensity without addition of drug, I_t is the fluorescence intensity after addition of each concentration of drug and I_{tot} is the fluorescence intensity after complete vesicle permeabilization, by addition of polidocanol [38].

3. Results and Discussion

3.1 PE limits the formation of GUVs

Aiming to mimic the inner membrane of *E. coli*, the preparation of GUVs composed of its main lipids, namely PE and PG, was attempted. To inspect the effect of lipid structure and/or charge, mixed compositions were also tested.

Using a solution containing only PC allowed the effective formation of GUVs, with a great number of vesicles (Figure 8, top left). GUVs formed with PC were varied in size (Figure 9). These results are in line with previous literature [15].

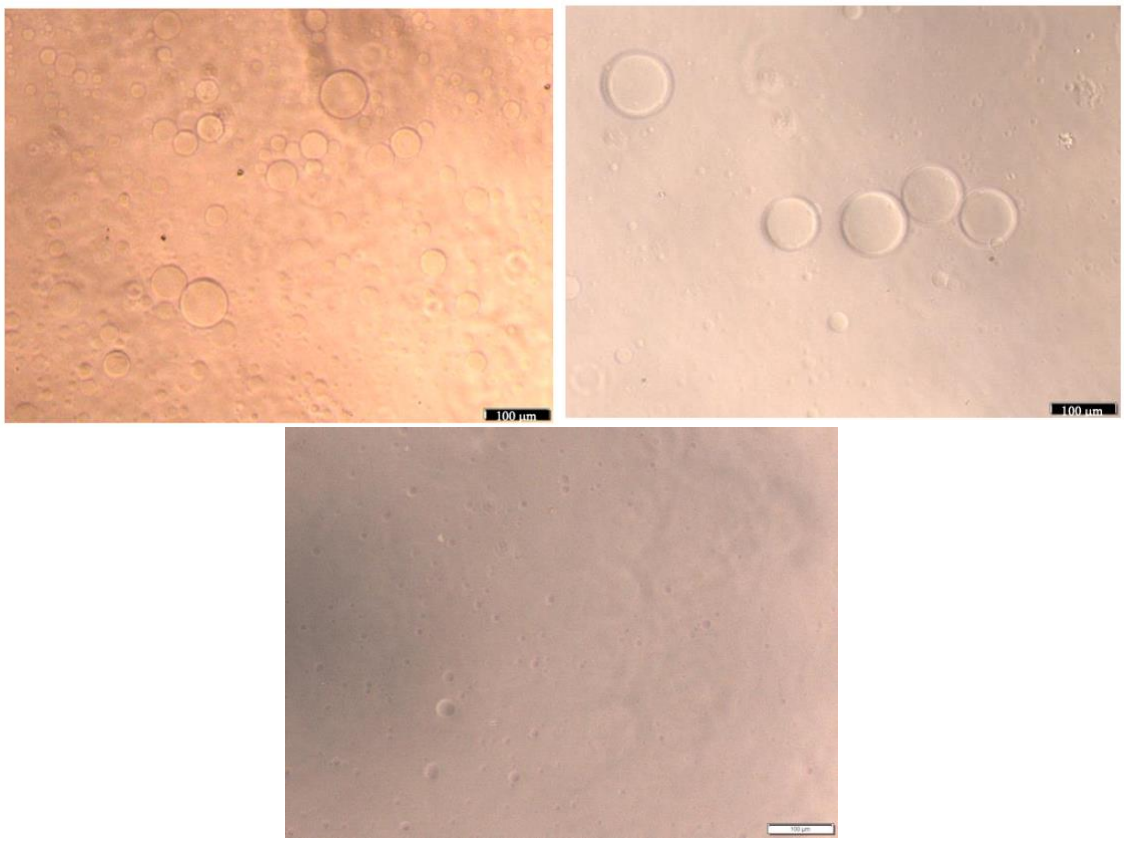

Figure 8: Example images of GUVs formation, 100% PC on the top left, 100% PG on the top right and 20% PE – 80% PG on the bottom.

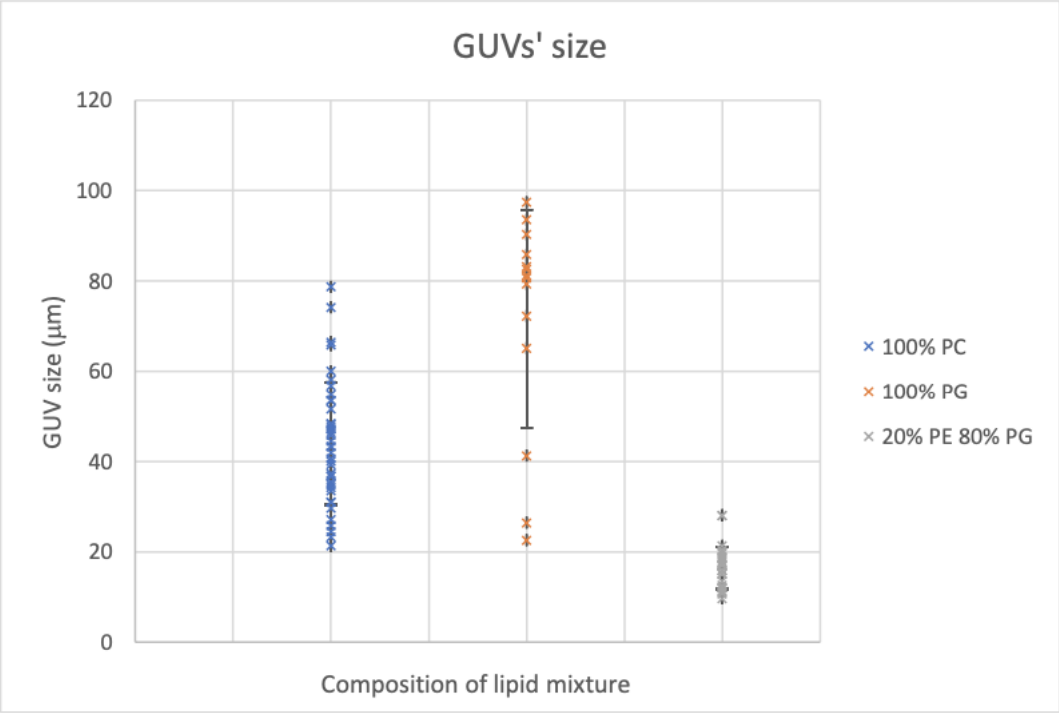

Figure 9: GUVs' size distribution. 100%PC resulted in a great variation in size, 100% PG resulted in bigger vesicles and 20% PE 80% PG resulted in smaller and less polydisperse vesicles.

Using only PG, resulted in the formation of a lower number of GUVs, but larger in size than those formed by PC (Figure 8, top right, and Figure 9). This difference in size can be explained by the larger headgroup of the anionic PG compared to that of PC [53, 54].

On the contrary, assays using 100% PE lipid composition did not result in any GUV formation. Although PC and PE are both lipids present in membrane bilayers and have been equated in biological systems, the smaller head group of PE, gives the lipid a conic shape, that might affect the formation of bilayers on its own [55]. Similarly, assays with 80% of PE and 20% of PG lipid composition (the most similar to that found in *E. coli's* inner membrane), and 50% PE/50% PG did not result in any GUV formation, as well. Only the 20% PE/80% PG ratio was successful in the formation of GUVs. Many vesicles were formed, but these were smaller in size compared to the ones formed by PC or PG only (Figure 8, bottom, and Figure 9). Since the inclusion of PE in more than 20% hampered the formation of GUVs, it can be concluded that PE acts as a limiting reagent in the vesicle's formation (in combination with PG).

3.2 Higher Concentrations of NAMs can Internalize GUVs

As the 20% PE – 80% PG is the composition most similar to the bacterial inner membrane, these were used for the assay. After the successful formation, the NAMs were added to the well. The formation of GUVs composed of PE was confirmed by visualization using an epifluorescence microscope equipped with a red filter, as PE is marked with rhodamine (Figure 10). Additionally, using the FITC filter, it is possible to determine if there was any entry of NAMs into the GUVs, as they should appear green.

With the lowest concentration of the NAMs (2 μM), there was no perceptible entry into the GUVs (Figure 10).

With higher concentrations of NAMs (15 μM, 30 μM and 60 μM), it appears that NAMs were capable of internalizing some of the vesicles, as some GUVs appear green. Still, not all of the vesicles were internalized, as some appear black in the green filter (Figure 10). Interestingly, most of the bright red GUVs appear darker in the green filter, which might indicate that, as they have a higher concentration of PE, this lipid is hindering the diffusion of NAMs.

Even though resorting to fluorescence microscopy gives us an indication that NAMs can internalize liposomes to some extent, they do not give us any indication on the partition of the NAMs and quantitative permeabilization capacity and how it is affected by the lipid composition. Likewise, the results obtained can be complemented by Permeabilization and Partition assays.

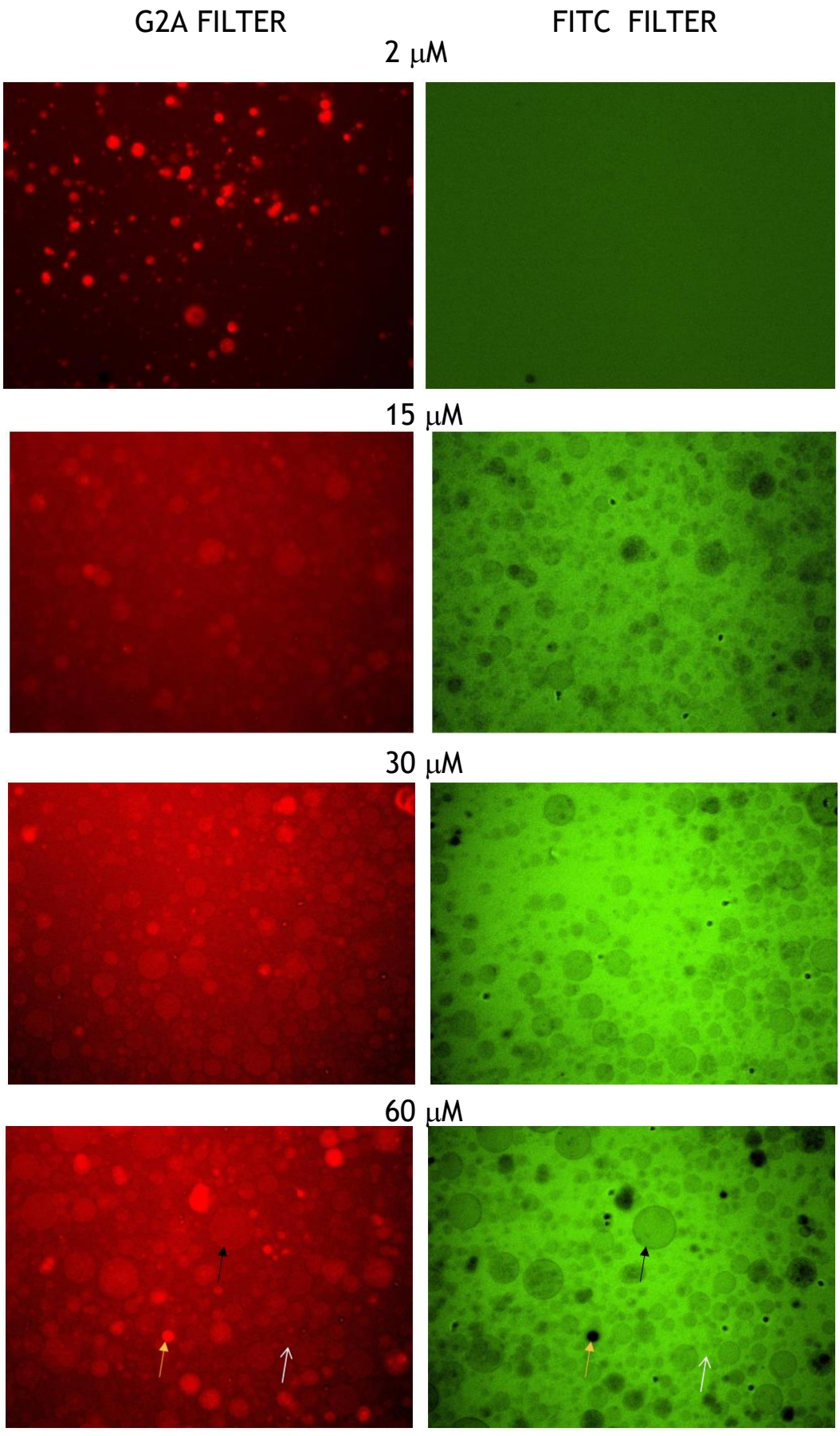

Figure 10: GUVs formed with 20% PE and 80% PG lipid composition, after the addition of NAMs (2, 15, 30 and 60 μM), visualized using the G2A filter (left) and FITC filter (right). The black arrow points to a GUV with internalization of NAMs, the white arrow to a GUV with low internalization of NAMs and the yellow arrow to a GUV without internalization of NAMs.

3.3 NAMs Show No Partition Towards Lipidic Membranes

Considering previous results, liposomes composed of PG (as the anionic model), and PC (as the zwitterionic model) were prepared, in order to evaluate the influence of different net charges on the partition of NAMs with lipidic membranes. Moreover, to more directly compare the partition results obtained with the permeabilization assays, LUVs were used instead of GUVs, given that a different protocol had to be followed for the encapsulation of PTS, key component of the permeabilization assays.

The mean diameter of the vesicles, determined by dynamic light scattering, was ca. 113 nm (polydispersity index 0.06) for PC and ca. 108 nm (polydispersity index 0.09) for PG. Steady-state fluorescence was used to determine the partition of NAMs, as well as other two antibiotics (CPX and PMB) used as controls known to have low, for CPX, and high, for PMB, interaction. [38, 56]. The concentration used for these antibiotics was 10 and 90 μM, respectively, following previous protocols [38, 57]. Tests were conducted in order to optimize the concentration used in these assays for NAMs, as high concentrations have a fluorescence that can saturate the equipment and low concentrations may not be sufficient to observe a shift. Additionally, spectroscopic assays do not need NAMs concentrations as high as those needed for microscopic assays, which depend on the molecule's accumulation for the visualization. The fluorescence intensity at the maximum emission wavelength was used to calculate the K_p. The results are summarized in Table 3.

Fluorescence quenching was observed for both PC and PG systems interacting with CPX (Figure 11, Plot A and B). K_p of 3.31± 0.18 and 3.15±0.07 were obtained for CPX partitioning with PC and PG vesicles, respectively. Such values point to a low and similar partition of CPX in both lipids. The behaviour observed and the constants obtained are in line with previously reported values (from 2.5 up to 3) [38, 58-60]. In fact, even though CPX is active against Gram-negative and Gram-positive bacteria, it is known that it has been classified as a low permeability substance and it is unlikely to cross the bacterial envelope via diffusion through the lipid membranes [38].

The K_p obtained for PMB were very similar to those encountered for CPX (3.40 ± 0.39 for the PC system and 3.37 ± 0.30 for the PG system). Such finding indicates a similar level of partition to that of CPX, but with different behaviours as in PC PMB seems to cause fluorescence enhancement as opposed to quenching (Figure 11, Plot C). Higher partition coefficients are described in the literature for PMB in vesicles of different compositions. The lower coefficient obtained in this study might be due to the use of a tagged antibiotic (PMB tagged to rhodamine), as the fluorophore can affect the interaction with the membrane and the subsequent diffusion. As a positively charged antimicrobial peptide, interaction with PG vesicles (anionic) is expected, due to electrostatic forces. Regarding PC (zwitterionic), the interaction with PMB can be explained by the repulsion of the positive charged end group of the choline towards the aqueous phase, exposing the hydrophobic region of the lipid for the interaction with the molecule. It is also possible for the molecule to insert itself into the membrane by establishing hydrophobic interactions [40, 56].

It was not possible to determine partition constants for the NAMs, given that it causes little to no signal variation with increasing lipid concentrations. However, a tendency for quenching can be observed for PG vesicles (Figure 11, Plot F), which might indicate that NAMs have a slight, albeit very small, partition in PG membranes that cannot be quantified. This could be explained by the ability of PG to form hydrogen bridges, due to the OH headgroup. It is also worth mentioning that one of the replicates was not in accordance with the other two, given that signal enhancement was observed as opposed to quenching. This might indicate that NAMs are capable of causing both types of shifts and, as such, interact differently (when they do) with the membrane. Still, more replicates are needed to further understand the results obtained.

Table 2: The partition constant, expressed as log (K_p)±SD for CPX, PMB and NAMs to PC and PG liposomes.

	PC	PG
CPX	3.31±0.18	3.15±0.07
PMB	3.40±0.39	3.37±0.30
NAMs	ND[a]	ND[a]

[a] Not possible to determine (Not determined, ND) with the experimental data obtained.

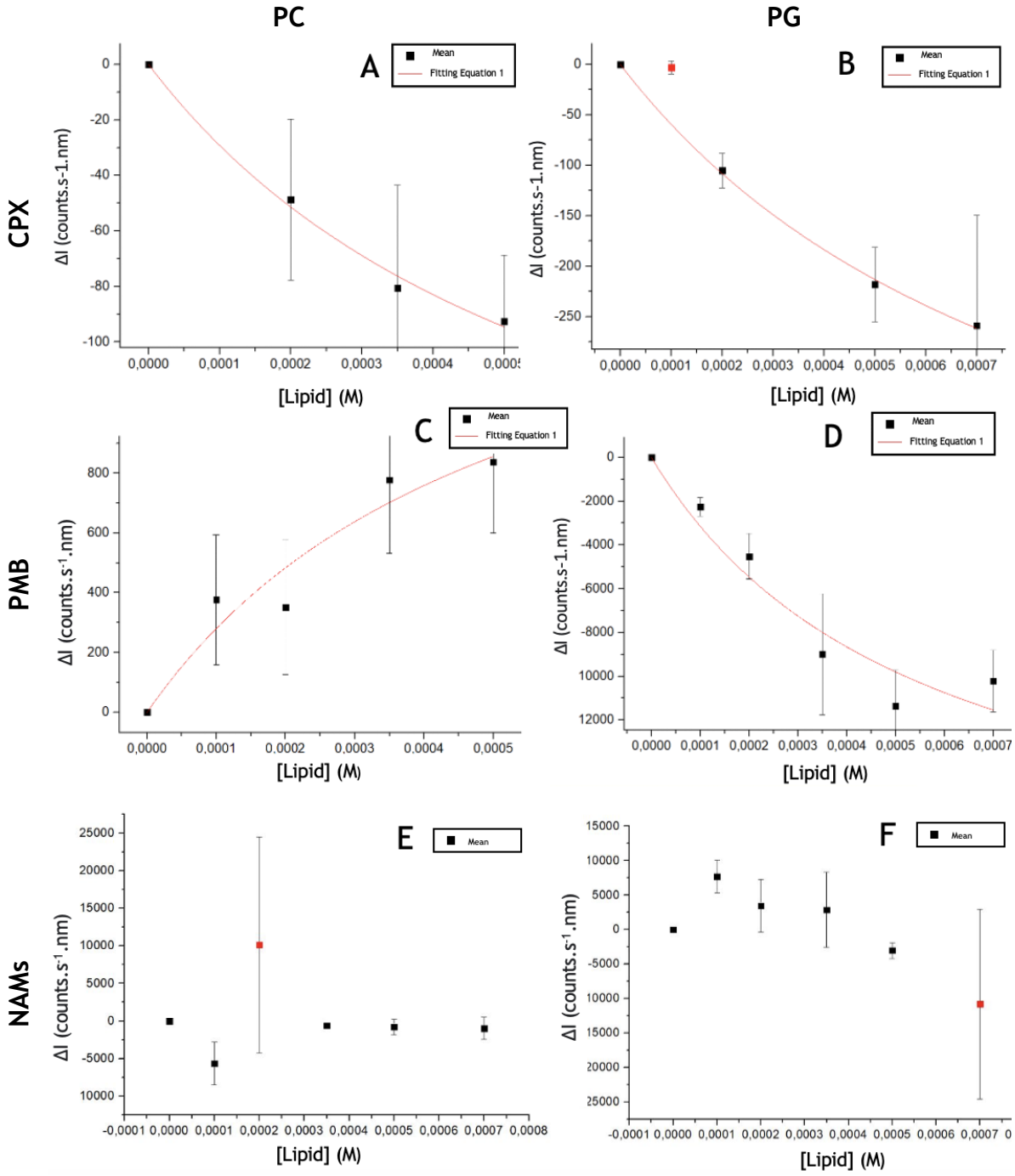

Figure 11: Determination of Kp from Steady-state fluorescence by fitting Equation 1. Variation of the fluorescence at emission maximum for CPX, PMB and NAMs upon addition of increasing amounts of PC and PG from 0 to 700 μM. Error bars represent the standard deviation (SD) of three independent experiments. Graphs A and B corresponds to CPX; C and D to PMB; E and F to NAMs. A, C and E use PC vesicles and B,D and F PG vesicles.

3.4 NAMs Permeabilization results show variability

To further clarify the ability of NAMs to internalize lipidic membranes, the fluorophore/quencher pair assay was performed. Briefly, the leakage and subsequent quenching of the fluorescent probe – PTS – encapsulated in LUVs was followed, which can be directly correlated with the ability of the molecule to permeabilize the lipid bilayer. CPX and PMB, whose behaviour is already described in literature, were used as controls for permeabilization. The concentrations studied (0, 5, 10, 15, 20 μM for CPX; 0, 5, 30, 90, 200 μM for PMB, and 0, 5, 10, 15, 20 μM for NAMs) were defined following similar studies for CPX and PMB, and following what was obtained from the microscopic assay and Partition assays in the case of NAMs [38, 57].

PTS-loaded LUVs were prepared, and their size checked by DLS. An average size of 118 nm (polydispersity index = 0.16) was obtained for PG vesicles, and an average size of 124 nm (polydispersity index = 0.12) was obtained for PC vesicles.

Upon fluorescence intensity measurements, the signal increased with antibiotic/NAMs' concentration increase, confirming that the antibiotic was emitting at the elected wavelength. Therefore, the fluorescence signal of the antibiotic in the same conditions but without the presence of LUVs, as well as the signal from the MV alone and polidocanol alone were measured and subtracted from the samples. In Table 3, there are the results for the mean of intensity with the references subtracted, and the percentage of leakage for each concentration.

For CPX, in PC vesicles, it was not possible to calculate a reasonable percentage of leakage, as we did not find a linear tendency with concentration increase after removal of the reference's signals. However, analyzing only the mean fluorescence intensity for each concentration (i.e., without the references subtracted), in Table 4 in Annex 2, there is a tendency for decrease. These results likely indicate a reduced permeabilization capacity of CPX in PC membranes, which is in line with reported results [38]. In PG, the third and last value of the %Leakage (22.5% and 30.4%, corresponding to concentrations of 20

and 40 μM, respectively in Table 3) are reasonable values for this assay [38]. It is important to note that a lot of variability was found between replicates. A clear explanation for this phenomenon is not possible. However, it is possible that the interaction between the lipids and the antibiotics is causing spectroscopic shifts that influence the signal measured. This might also explain why the signal observed for the sample without antibiotic addition was lower compared to those with antibiotic.

For PMB, the same issues with antibiotic signal disturbance were encountered. Still, it was possible to observe a clear decrease in fluorescence, in both lipidic systems, correlating with an increase of the percentage of leakage. This indicates a good permeabilization of the molecule, as expected [57].

For NAMs, there was a high variation in the values obtained which could be explained by an eventual interaction with the lipids that provokes a shift depending on the concentration. Additionally, and similarly to CPX, there seems to be a tendency for signal decrease with the three highest concentrations of NAMs when only looking at the samples and ignoring the references with polidocanol (Table 4, Annex 2).

These results clearly show that the permeabilization assays need to be optimized as several issues were identified: i) inability to determine the true concentration of lipid in the samples; ii) fluorescence signal from the antibiotics, MV and polidocanol at the WLs used. Moreover, from the chromatogram obtained, the maximum signal observed for the PTS-loaded LUVs (without dilution) was ~5000, as seen in the chromatograms in Annex 1. Inherently, by diluting the LUVs to 200 μM in the samples the fluorescence signals to be read are substantially lower and might be too low to discriminate differences with the needed sensitivity. Possibly, the concentration of PTS-loaded LUVs needs to be increased.

Table 3: Results of the Permeabilization assay (Mean of Fluorescence Intensity of three assays, with references subtracted, and %Leakage) for CPX, PMB and NAMs for both systems (PC and PG vesicles).

	Concentration (μM)	Ī	%Leakage	Ī	%Leakage
		PC		PG	
CPX	0	-884	0	-970	0
	5	4574	-701	668	-156.6
	10	7493	1276	-173	22.5
	15	6602	-570	-143	68.5
	20	5112	848	208	30.4
PMB	0	-989	0	-807	0
	5	1065	118	1094	84.2
	30	834	140.2	698	134.4
	90	475	133.9	1046	176.5
	120	139	156.2	861	2353.4
NAMs	0	-784	0	-926	0
	5	1239	257	-5778	-5318
	10	1682	-214	958	148
	15	1273	103	794	130
	20	1069	-177	-751	8

Conclusion and Future Work

Optimization of the production of Giant Unilamellar Vesicles (GUVs) was carried out, with successful formation of vesicles for lipid compositions of 100% PC, 100% PG and 20% PE – 80% PG. 100% PC formed vesicles with polydisperse size (43.2 ± 12.8 μm), while 100% PG composition resulted in larger (81 ± 24.2 μm) yet fewer vesicles, which might be explained by its cylindric shape. The 20% PE – 80% PG composition resulted in the formation of many but small vesicles (size). The lipid compositions of 100% PE and the mix of 50% PE and 50% PG were unsuccessful in the formation of GUVs, indicating that the presence of PE in high relative amounts (50% or more) limits the formation of GUVs, most likely due to PE's conical shape.

Microscopy assays to assess whether fluorescently labelled NAMs could cross the GUVs were conducted with different NAMs' concentrations. For the lowest concentration (2 μM) no internalization was observed. With higher concentrations (15, 30 and 60 μM) internalization was observed to some extent.

Spectroscopic assays – Partition and Permeabilization assays – were also carried out to further investigate NAMs interaction with the membranes and the influence of the lipid charge. Two other antibiotics (CPX and PMB) for which similar studies have been performed were used as controls. It was not possible to quantify the partition of NAMs. However, there seems to be a slightly higher interaction with PG vesicles than PC vesicles, due to its anionic charge. Permeabilization assays results for NAMs showed high variation intraassay (i.e., there was not a linear tendency with concentration increase) and between replicates, which could be explained by different shifts happening depending on the concentration. Once more, in PG vesicles, a tendency of decrease could be observed, which can point to some permeabilization capacity.

To conclude, NAMs internalization in liposomes could be visualized (with the higher concentrations used) to some extent but its interaction, partition and permeabilization, with anionic and zwitterionic vesicles point to little to no interaction with the membrane. Therefore, the introduction of mechanisms

as delivery vehicles in combination with NAMs seems the most promising approach to increase the internalization of the probes. Both partition and permeabilization assays could be employed to evaluate if the chosen carrier or a panel of carriers is effective for delivery, using both anionic and zwitterionic vesicles, and, in a later stage, compositions of lipid that mimic the membrane more accurately.

Additionally, given the high variability obtained in the permeabilization assays, which hypothetically could be due to shifts happening, partition studies with different antibiotics' concentration could be carried out to better understand the results. Other possibilities for future work are the study of the outer membrane, study of the limiting elements of the membrane for the diffusion of NAMs and development of carriers for NAMs.

References

1. Ang, J.Y., E. Ezike, and B.I. Asmar, *Antibacterial resistance*. Indian J Pediatr, 2004. **71**(3): p. 229-39.
2. Batchelder, J.I., P.J. Hare, and W.W.K. Mok, *Resistance-resistant antibacterial treatment strategies*. Front Antibiot, 2023. **2**.
3. Antimicrobial Resistance, C., *Global burden of bacterial antimicrobial resistance in 2019: a systematic analysis*. Lancet, 2022. **399**(10325): p. 629-655.
4. Prestinaci, F., P. Pezzotti, and A. Pantosti, *Antimicrobial resistance: a global multifaceted phenomenon*. Pathog Glob Health, 2015. **109**(7): p. 309-18.
5. Levy, S.B. and B. Marshall, *Antibacterial resistance worldwide: causes, challenges and responses*. Nat Med, 2004. **10**(12 Suppl): p. S122-9.
6. Munita, J.M. and C.A. Arias, *Mechanisms of Antibiotic Resistance*. Microbiol Spectr, 2016. **4**(2).
7. Nacher-Vazquez, M., et al., *The role of Nucleic Acid Mimics (NAMs) on FISH-based techniques and applications for microbial detection*. Microbiol Res, 2022. **262**: p. 127086.
8. Santos, R.S., et al., *Nanomaterials and molecular transporters to overcome the bacterial envelope barrier: Towards advanced delivery of antibiotics*. Adv Drug Deliv Rev, 2018. **136-137**: p. 28-48.
9. Santos, R.S., et al., *Effect of Native Gastric Mucus on in vivo Hybridization Therapies Directed at Helicobacter pylori*. Molecular Therapy-Nucleic Acids, 2015. **4**.
10. Cerqueira, L., et al., *DNA mimics for the rapid identification of microorganisms by fluorescence in situ hybridization (FISH)*. Int J Mol Sci, 2008. **9**(10): p. 1944-60.
11. Karkare, S. and D. Bhatnagar, *Promising nucleic acid analogs and mimics: characteristic features and applications of PNA, LNA, and morpholino*. Appl Microbiol Biotechnol, 2006. **71**(5): p. 575-86.
12. Nielsen, P.E., et al., *Sequence-selective recognition of DNA by strand displacement with a thymine-substituted polyamide*. Science, 1991. **254**(5037): p. 1497-500.
13. Agnieszka A. Zuber, E.K., Akash Bachhuka, *3.06 - Biosensing*. Comprehensive Nanoscience and Nanotechnology (Second Edition), 2019: p. Pages 105-126.
14. Yoo, B.H., et al., *2 '-O-methyl-modified phosphorothioate antisense oligonucleotides have reduced non-specific effects in vitro*. Nucleic Acids Research, 2004. **32**(6): p. 2008-2016.
15. Pereira, D.A., et al., *Imaging of photoacoustic-mediated permeabilization of giant unilamellar vesicles (GUVs)*. Scientific Reports, 2021. **11**(1).
16. Morris, M.C., et al., *A non-covalent peptide-based carrier for in vivo delivery of DNA mimics*. Nucleic Acids Res, 2007. **35**(7): p. e49.
17. Silhavy, T.J., D. Kahne, and S. Walker, *The Bacterial Cell Envelope*. Cold Spring Harbor Perspectives in Biology, 2010. **2**(5).
18. Vollmer, W., D. Blanot, and M.A. de Pedro, *Peptidoglycan structure and architecture*. Fems Microbiology Reviews, 2008. **32**(2): p. 149-167.
19. Cooper, G.M., *The cell : a molecular approach*. Eighth edition. ed. 2019, New York: Oxford University Press.
20. Yang, S.T., et al., *The role of cholesterol in membrane fusion*. Chem Phys Lipids, 2016. **199**: p. 136-143.

21. Wilson, J.H. and T. Hunt, *Molecular biology of the cell, 4th edition : a problems approach*. 2002, New York ; London: Garland Science. xxii, 711 p. : ill.
22. Melton, L., F. Shahidi, and P. Varelis, *Encyclopedia of food chemistry*. 2019, Amsterdam: Elsevier.
23. Li, J., et al., *A review on phospholipids and their main applications in drug delivery systems.* Asian Journal of Pharmaceutical Sciences, 2015. **10**(2): p. 81-98.
24. Drescher, S. and P. van Hoogevest, *The Phospholipid Research Center: Current Research in Phospholipids and Their Use in Drug Delivery.* Pharmaceutics, 2020. **12**(12).
25. Terao, J., et al., *Structural-Analysis of Hydroperoxides Formed by Oxidation of Phosphatidylcholine with Singlet Oxygen.* Lipids, 1981. **16**(6): p. 427-432.
26. Paltauf, F. and A. Hermetter, *Phospholipids - Natural, Semisynthetic, Synthetic.* Phospholipids, 1990: p. 1-12.
27. Laouini, A., et al., *Preparation, Characterization and Applications of Liposomes: State of the Art.* Journal of Colloid Science and Biotechnology, 2012. **1**(2): p. 147-168.
28. Zhirnov, A.E., et al., *Lipid composition determines interaction of liposome membranes with Pluronic L61.* Biochimica Et Biophysica Acta-Biomembranes, 2005. **1720**(1-2): p. 73-83.
29. Niehage, C., et al., *Liposome-Based Assays to Study Membrane-Associated Protein Networks.* Endosome Signaling, Pt A, 2014. **534**: p. 223-243.
30. Frick, M., C. Schwieger, and C. Schmidt, *Liposomes as Carriers of Membrane-Associated Proteins and Peptides for Mass Spectrometric Analysis.* Angewandte Chemie-International Edition, 2021. **60**(20): p. 11523-11530.
31. Nakhaei, P., et al., *Liposomes: Structure, Biomedical Applications, and Stability Parameters With Emphasis on Cholesterol.* Frontiers in Bioengineering and Biotechnology, 2021. **9**.
32. Ali Demir, S., S. Ali Demir, and A.D. Sezer, *Application of Nanotechnology in Drug Delivery*. 2014, Place of publication not identified: IntechOpen.
33. Pattni, B.S., V.V. Chupin, and V.P. Torchilin, *New Developments in Liposomal Drug Delivery.* Chemical Reviews, 2015. **115**(19): p. 10938-10966.
34. Pattni, B.S., V.V. Chupin, and V.P. Torchilin, *New Developments in Liposomal Drug Delivery.* Chem Rev, 2015. **115**(19): p. 10938-66.
35. Bhatia, T., et al., *Preparing giant unilamellar vesicles (GUVs) of complex lipid mixtures on demand: Mixing small unilamellar vesicles of compositionally heterogeneous mixtures.* Biochimica Et Biophysica Acta-Biomembranes, 2015. **1848**(12): p. 3175-3180.
36. Rodrigues, C., et al., *Spectrophotometric determination of drug partition coefficients in dimyristoyl-L-alpha-phosphatidylcholine/water: a comparative study using phase separation and liposome suspensions.* Analytica Chimica Acta, 2001. **428**(1): p. 103-109.
37. Rice, J.E. and ScienceDirect, *Organic chemistry concepts and applications for medicinal chemistry*. 2014, San Diego, CA: Academic Press, an imprint of Elsevier.
38. Sousa, C.F., et al., *Passive Diffusion of Ciprofloxacin and its Metalloantibiotic: A Computational and Experimental study.* J Mol Biol, 2021. **433**(9): p. 166911.
39. Matos, C., C. Moutinho, and P. Lobao, *Liposomes as a model for the biological membrane: studies on daunorubicin bilayer interaction.* J Membr Biol, 2012. **245**(2): p. 69-75.

40. Cetuk, H., et al., *Partitioning of Seven Different Classes of Antibiotics into LPS Monolayers Supports Three Different Permeation Mechanisms through the Outer Bacterial Membrane.* Langmuir, 2021. **37**(4): p. 1372-1385.
41. Rodrigues, C., et al., *Interaction of grepafloxacin with large unilamellar liposomes: Partition and fluorescence studies reveal the importance of charge interactions.* Langmuir, 2002. **18**(26): p. 10231-10236.
42. Catarina Rodrigues, P.G., Salette Reis, J. L. F. C. Lima, and Baltazar de Castro, *Derivative spectrophotometry as a tool for the determination of drug partition coefficients in water dimyristoyl-L—phosphatidylglycerol DMPG ž /liposomes.* Biophysical Chemistry, 2001. **94 (2001)**: p. 97-106.
43. Çağdaş, M., *Liposomes as Potential Drug Carrier Systems for Drug Delivery*. 2014, sine loco: IntechOpen.
44. Nasr, G., et al., *Liposomal membrane permeability assessment by fluorescence techniques: Main permeabilizing agents, applications and challenges.* International Journal of Pharmaceutics, 2020. **580**.
45. Manzini, M.C., et al., *Peptide:lipid ratio and membrane surface charge determine the mechanism of action of the antimicrobial peptide BP100. Conformational and functional studies.* Biochim Biophys Acta, 2014. **1838**(7): p. 1985-99.
46. Reyna, D.E. and E. Gavathiotis, *Liposomal Permeabilization Assay to Study the Functional Interactions of the BCL-2 Family.* Methods Mol Biol, 2019. **1877**: p. 111-119.
47. Ben Trad, F., et al., *Electrochemiluminescence Imaging of Liposome Permeabilization by an Antimicrobial Peptide: Melittin.* Chemical & Biomedical Imaging, 2023. **1**(1): p. 58-65.
48. Aguilera, J., S. Vazquez-Reyes, and J.J. Sun, *A Fluorescence Dequenching-based Liposome Leakage Assay to Measure Membrane Permeabilization by Pore-forming Proteins.* Bio-Protocol, 2021. **11**(10).
49. Miranda, D. and J.F. Lovell, *Mechanisms of Light-induced Liposome Permeabilization.* Bioeng Transl Med, 2016. **1**(3): p. 267-276.
50. Mayer, L.D., M.J. Hope, and P.R. Cullis, *Vesicles of variable sizes produced by a rapid extrusion procedure.* Biochim Biophys Acta, 1986. **858**(1): p. 161-8.
51. Santos, N.C., M. Prieto, and M.A. Castanho, *Quantifying molecular partition into model systems of biomembranes: an emphasis on optical spectroscopic methods.* Biochim Biophys Acta, 2003. **1612**(2): p. 123-35.
52. Bartlett, G.R., *Phosphorus assay in column chromatography.* J Biol Chem, 1959. **234**(3): p. 466-8.
53. Boudiere, L., et al., *Glycerolipids in photosynthesis: composition, synthesis and trafficking.* Biochim Biophys Acta, 2014. **1837**(4): p. 470-80.
54. Dickey, A. and R. Faller, *Examining the contributions of lipid shape and headgroup charge on bilayer behavior.* Biophys J, 2008. **95**(6): p. 2636-46.
55. Vance, D.E. and J.E. Vance, *Biochemistry of lipids, lipoproteins and membranes*. 2008, Amsterdam: Elsevier. p.
56. Domingues, M.M., et al., *Biophysical characterization of polymyxin b interaction with LPS aggregates and membrane model systems.* Biopolymers, 2012. **98**(4): p. 338-344.
57. Domingues, M.M., et al., *Biophysical characterization of polymyxin B interaction with LPS aggregates and membrane model systems.* Biopolymers, 2012. **98**(4): p. 338-44.
58. Ferreira, M., et al., *Fluoroquinolone Metalloantibiotics: A Promising Approach against Methicillin-Resistant Staphylococcus aureus.* Int J Environ Res Public Health, 2020. **17**(9).

59. Ribeiro, C., S.C. Lopes, and P. Gameiro, *New insights into the translocation route of enrofloxacin and its metalloantibiotics.* J Membr Biol, 2011. **241**(3): p. 117-25.
60. Ferreira, M., C.F. Sousa, and P. Gameiro, *Fluoroquinolone Metalloantibiotics to Bypass Antimicrobial Resistance Mechanisms: Decreased Permeation through Porins.* Membranes (Basel), 2020. **11**(1).

Annexes

Annex 1: Chromatograms

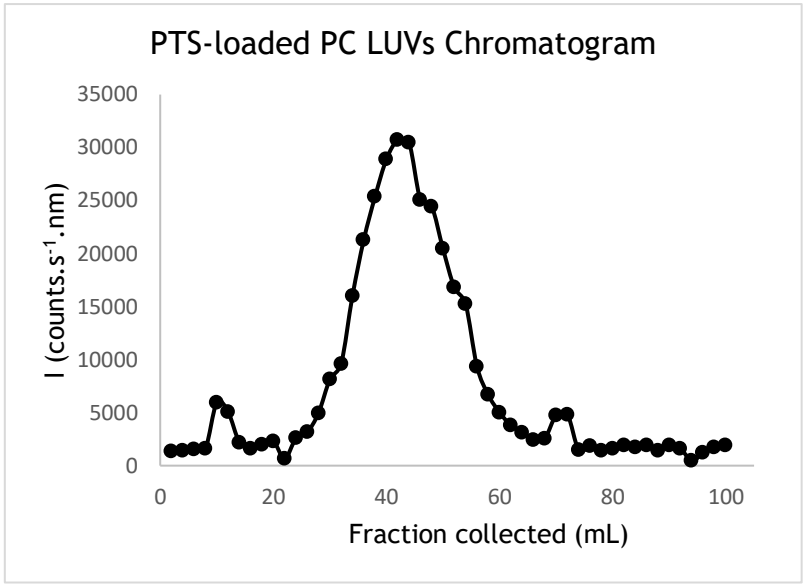

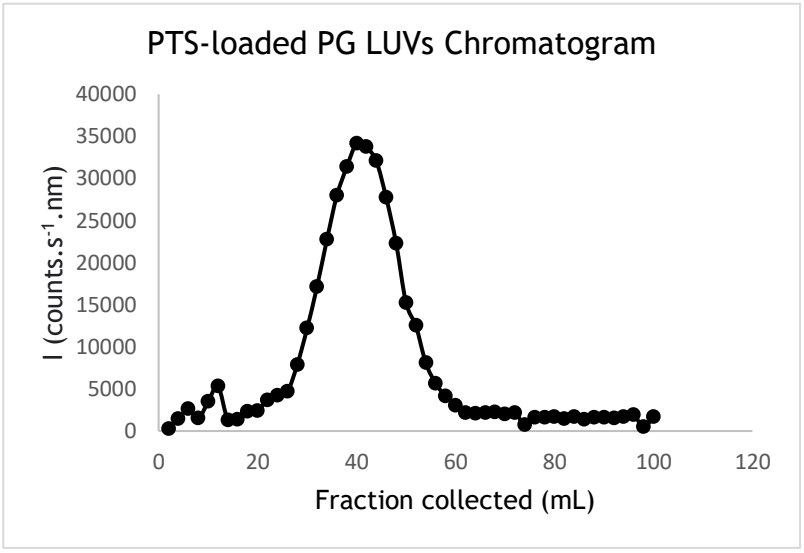

Figure 12: Chromatograms for both systems (PC and PG vesicles) elution. The first peak corresponds to the PTS-loaded LUVs and the second peak to free PTS molecules.

Annex 2: Permeabilization Results without references

Table 4: Permeabilization Results, mean of intensity of fluorescence of three assays without references subtracted, for CPX, PMB and NAMs in both systems used (PC and PG).

	Concentration (µM)	$\bar{I}$	
		PC	PG
CPX	0	-884	-970
	5	4574	668
	10	7493	-173
	15	6602	-143
	20	5112	208
PMB	0	-989	-807
	5	1065	1094
	30	834	698
	90	475	1046
	120	139	861
NAMs	0	-784	-926
	5	1239	-5778
	10	1682	958
	15	1273	794
	20	1069	-751